Int. J. Anal. Appl. (2024), 22:31

International Journal of Analysis and Applications

A Kinetic Non-Steady-State Analysis of Immobilized Enzyme Systems Without External Mass Transfer Resistance

M. Sivakumar[1], M. Mallikarjuna[2], R. Senthamarai[2,*]

[1]*Department of Mathematics, College of Science and Humanities, SRM Institute of Science and Technology, Vadapalani, Chennai - 600026, Tamilnadu, India*
[2]*Department of Mathematics, College of Engineering and Technology, SRM Institute of Science and Technology, Kattankulathur – 603 203, Tamilnadu, India*

[*]*Corresponding author:* senthamr@srmist.edu.in

Abstract. In this paper, a non-steady-state non-linear reaction diffusion in immobilized enzyme on the nonporous medium is considered for its mathematical analysis. The non-linear terms in this model are related to the Michaelis-Menten kinetics. For the considered model, the approximate analytical expressions of the substrate concentration and the effectiveness factor for the various geometric profiles of immobilized enzyme pellets are obtained using homotopy perturbation method (HPM). The obtained approximate analytical expressions proved to be fit for all values of parameters. Numerical solutions are also provided using the MATLAB software. When comparing the analytical and the numerical solutions, satisfactory results are noted. The effects of Thiele modulus and Michaelis-Menten kinetic constants on the effectiveness factor are also analyzed.

1. Introduction

The process of immobilizing the enzymes on the support materials has its extended use in the continues bioreactors and batch reactors. Immobilized enzymes exhibit distinct kinetic behaviours due to factors such as diffusion limitations within and between particles, substrate distribution between the support and the surrounding solution, structural changes during immobilization, and microenvironmental alterations stemming from support interactions, leading to deviations from the intrinsic kinetics observed in free enzymes. The extent of these effects is contingent on the characteristics of the support material, the nature of the substrate and its concentration, and the specifics of the immobilization technique employed. [1–3]. Mass transfer limitations impacting the

Received: Nov. 15, 2023.

2020 *Mathematics Subject Classification.* 97M60, 35A35, 35A22, 35G31.

Key words and phrases. Mathematical modelling; Non-linear reaction-diffusion equations; Michaelis-Menten kinetics; homotopy perturbation method.

https://doi.org/10.28924/2291-8639-22-2024-31
ISSN: 2291-8639

observed reaction rates stem from two key factors: external mass transfer resistance, which hinders the transport of substrate from the bulk fluid phase to the external surface of support pellets, and internal mass transfer resistances associated with pore diffusion [4,5]. For the design, modelling, simulation, and process of development of batch reactors, a crucial step involves studying the intrinsic kinetics of enzymatic reactions. This involves a better understanding of the reaction kinetics without the interference of mass transfer constraints [6].

In recent times, researchers prefer the analytical solution for non-linear differential equations since it offers a distinct advantage over numerical solutions by providing precise, closed-form expressions, enabling deeper insights into the underlying mathematics and yielding results that can be rigorously proven and interpreted, which is essential for advancing our understanding of the system. Karthika et al. [7] utilized the homotopy perturbation method for obtaining the analytical expression for the mathematical model of packed bed tubular reactor for lactose hydrolysis. Praveen et al. [8] provided analytical expressions for the immobilized enzymes with the competitive and uncompetitive substrate and product inhibitions with the reversible Michaelis-Menten reactions by utilizing the modified Adomian decomposition method for all the possible values of the presented parameters. The analytical expressions for effectiveness factor of batch reactor performance are also presented and analysed. Jeyabarathi et al. [9] utilized the semi-analytical methods namely Adomian decomposition method and Taylors series method for solving the non-linear differential equation arising in the reaction diffusion kinetic model of Langmuir-Hinshelwood-Hougen-Watson (LHHW) type for various geometries and the effectiveness factor. Sivakumar and Senthamarai [10,11] derived the substrate concentration of steady-state immobilized enzyme system with and without the mass transfer resistance for the various geometries of the catalytic pellets immobilized on to the nonporous medium. These approaches are limited to the steady-state conditions of the immobilized enzymes. To the authors best of the knowledge, there is no existing analytical expression for non-steady-state condition of reaction-diffusion kinetics of immobilized enzyme on the nonporous medium without the mass transfer resistance which can be used for the better understanding of the reaction kinetics of immobilized enzyme.

In this paper, the non-steady-state condition model of the substrate concentration of immobilized enzymes on the nonporous medium which is not affected by the mass transfer is analysed mathematically. The non-steady-state reaction-diffusion equation of the substrate concentration is a non-linear differential equation with the non-linear terms related to the Michaelis-Menten kinetics. The approximate analytical expressions for the substrate concentration with the geometries of planar, cylindrical and spherical pellets are obtained by utilizing the homotopy perturbation method and Laplace transform method for various values of parameters. The closed-form analytical expression of the effectiveness factors of planar, cylindrical, and spherical geometry of the enzyme pellet is also provided. Numerical solution of the system is obtained using the MATLAB software and are compared with the obtained analytical results.

2. Mathematical formulation of the model

A non-steady-state nonlinear differential equation with the initial and boundary conditions of substrate concentration of immobilized enzyme on the nonporous medium is considered and it is given as [12]:

$$\frac{\partial C(x,t)}{\partial t} = \frac{\partial^2 C(x,t)}{\partial x^2} + \frac{g-1}{x}\frac{\partial C(x,t)}{\partial x} - \frac{\alpha^2 C(x,t)}{1+\beta C(x,t)} \tag{2.1}$$

where

$$C(x,t) = 0 \text{ when } t = 0, \tag{2.2}$$

$$\frac{\partial C(x,t)}{\partial x} = 0 \text{ when } x = 0, \tag{2.3}$$

$$C(x,t) = 1 \text{ when } x = 1. \tag{2.4}$$

where $C(x,t)$ is the concentration of the substrate and α depict the Thiele modulus and β is the dimensionless Michaelis-Menten constant.

Further, to describe the mass transfer limitation effect on the overall reaction rate, the overall effectiveness factor η is derived by using

$$\eta = \frac{\text{reaction rate}}{\text{reaction rate in the absence of internal and external resistances}} \tag{2.5}$$

$$\eta = \frac{g(1+\beta)}{\alpha^2}\left(\frac{\partial C}{\partial x}\right)_{x=1} \tag{2.6}$$

3. An approximate analytical expression of the non-steady state concentration using HPM with Laplace transform technique

Nonlinear equations serve as essential tools for representing challenges across various domains, including applied mathematics, physics, chemical engineering, and biological sciences. The persistent challenge faced by researchers in these fields pertains to obtain the exact solutions. In recent years semi-analytical methods like homotopy perturbation method (HPM) [13] - [16], Akbari-Ganji method (AGM) [17] - [19], Taylor's series method [10, 11, 20, 21], Adomian decomposition method (ADM) [19, 22], variational iteration method (VIM) [23] - [25] are utilized for obtaining the approximate analytical solution.

In this article, we have utilized HPM and Laplace transform technique for obtaining the approximate analytical expression for the substrate concentration of immobilized enzyme on the nonporous material. The approximate analytical expression is obtained as follows (see Appendix A):

$$C(x,t) = \frac{\cosh\left(x\sqrt{\frac{a}{g}}\right)}{\cosh\left(\sqrt{\frac{a}{g}}\right)} - \pi\sum_{n=0}^{\infty}\frac{(2n+1)\cos\left(\frac{(2n+1)\pi}{2}x\right)e^{-gt\left(\frac{(2n+1)^2\pi^2}{4}+a\right)}}{\left(\frac{(2n+1)^2\pi^2}{4}+a\right)sin\left(\frac{(2n+1)\pi}{2}\right)} \tag{3.1}$$

where

$$a = \frac{\alpha^2}{1+\beta}$$

applying the solution (3.1) in (2.6), we will get the required effectiveness factor as

$$\eta = \frac{g(1+\beta)}{\alpha^2}\left[\sqrt{\frac{a}{g}}\tanh\sqrt{\frac{a}{g}} + \pi^2\sum_{n=0}^{\infty}\frac{\frac{(2n+1)^2}{2}e^{-gt\left(\frac{(2n+1)^2\pi^2}{4}+a\right)}}{\left(\frac{(2n+1)^2\pi^2}{4}+a\right)}\right] \tag{3.2}$$

4. Influence of geometry

4.1. **Planar geometry.** When $g = 1$, the pellet shape in Eq. (2.1) becomes planar and the resulting concentration flow is as follows:

$$C(x,t) = \frac{\cosh\left(x\sqrt{a}\right)}{\cosh\left(\sqrt{a}\right)} - \pi\sum_{n=0}^{\infty}\frac{(2n+1)\cos\left(\frac{(2n+1)\pi}{2}x\right)e^{-t\left(\frac{(2n+1)^2\pi^2}{4}+a\right)}}{\left(\frac{(2n+1)^2\pi^2}{4}+a\right)sin\left(\frac{(2n+1)\pi}{2}\right)} \tag{4.1}$$

and the corresponding effectiveness factor is obtained by taking $g = 1$ and applying (4.1) in (2.6), we get

$$\eta = \frac{(1+\beta)}{\alpha^2}\left[\sqrt{a}\tanh\sqrt{a} + \pi^2\sum_{n=0}^{\infty}\frac{\frac{(2n+1)^2}{2}e^{-t\left(\frac{(2n+1)^2\pi^2}{4}+a\right)}}{\left(\frac{(2n+1)^2\pi^2}{4}+a\right)}\right] \tag{4.2}$$

4.2. **Cylindrical geometry.** When $g = 2$, the pellet shape is a cylindrical geometry and the resulting concentration flow accordingly becomes

$$C(x,t) = \frac{\cosh\left(x\sqrt{\frac{a}{2}}\right)}{\cosh\left(\sqrt{\frac{a}{2}}\right)} - \pi\sum_{n=0}^{\infty}\frac{(2n+1)\cos\left(\frac{(2n+1)\pi}{2}x\right)e^{-2t\left(\frac{(2n+1)^2\pi^2}{4}+a\right)}}{\left(\frac{(2n+1)^2\pi^2}{4}+a\right)\sin\left(\frac{(2n+1)\pi}{2}\right)} \tag{4.3}$$

and the corresponding effectiveness factor is obtained by taking g =2 and applying (4.3) in (3.2), we get

$$\eta = \frac{2(1+\beta)}{\alpha^2}\left[\sqrt{\frac{a}{2}}\tanh\sqrt{\frac{a}{2}} + \pi^2\sum_{n=0}^{\infty}\frac{\frac{(2n+1)^2}{2}e^{-2t\left(\frac{(2n+1)^2\pi^2}{4}+a\right)}}{\left(\frac{(2n+1)^2\pi^2}{4}+a\right)}\right] \tag{4.4}$$

4.3. **Spherical geometry.** When $g = 3$, the pellet shape is a spherical geometry and the resulting concentration flow accordingly becomes

$$C(x,t) = \frac{\cosh\left(x\sqrt{\frac{a}{3}}\right)}{\cosh\left(\sqrt{\frac{a}{3}}\right)} - \pi\sum_{n=0}^{\infty}\frac{(2n+1)\cos\left(\frac{(2n+1)\pi}{2}x\right)e^{-3t\left(\frac{(2n+1)^2\pi^2}{4}+a\right)}}{\left(\frac{(2n+1)^2\pi^2}{4}+a\right)\sin\left(\frac{(2n+1)\pi}{2}\right)} \tag{4.5}$$

and the corresponding effectiveness factor is obtained by taking $g = 3$ and applying (4.5) in (3.2) and found as

$$\eta = \frac{3(1+\beta)}{\alpha^2}\left[\sqrt{\frac{a}{3}}\tanh\sqrt{\frac{a}{3}} + \pi^2\sum_{n=0}^{\infty}\frac{\frac{(2n+1)^2}{2}e^{-3t\left(\frac{(2n+1)^2\pi^2}{4}+a\right)}}{\left(\frac{(2n+1)^2\pi^2}{4}+a\right)}\right] \tag{4.6}$$

5. Result and discussion

5.1. **Planar geometry.** In non-steady state, the solution for a dimensionless substrate concentration has been derived for the model given by the Eq. (2.1) with its initial and boundary conditions Eqs. (2.2) - (2.4) by using HPM with Laplace transform and it resulted as Eq. (3.1) and its overall effectiveness factor η is expressed as Eq. (3.2) using Eq. (2.6). In particular, for the pellet shape factor value g = 1, the pellet geometry becomes a planar geometry and if we apply this factor value in Eq. (3.1) and Eq. (3.2), we have the non-steady state concentration Eq. (4.1) and its corresponding effectiveness factor Eq. (4.2) under this geometry. The dimensionless concentration profiles according to the planar geometrical results so obtained have clearly been demonstrated by the graphs given in Fig. 1 and the approximate analytical results obtained by HPM have been compared with their numerical simulation graphs plotted by the use of MATLAB software for various values of the parameters α, the Thiele modulus, β, the Michaelis-Menten diffusion constant and the time factor t to have a sense of ensuring how far our method of solution matches with the numerical simulations which will always better fit to the exact solutions. Here we could see that the approximate analytical results even in non-steady state are almost coinciding with the results of numerical simulations. In Table. 1, the mean errors have been calculated between the analytical solutions and the numerical solutions for which the parameter values have been collected from the previous articles and it describes that the approximate analytical solutions and the corresponding numerical results almost coincide under this geometry even in non-steady state. The dimensionless concentration levels and the overall effectiveness factor variations corresponding to the variations in concentration levels have been represented by the graphs, Figure. 1 and Figure. 2, under various values of the parameters by this geometry, with the help of MATLAB coding, that satisfies the characteristics of flows as per the Michaelis-Menten kinetics.

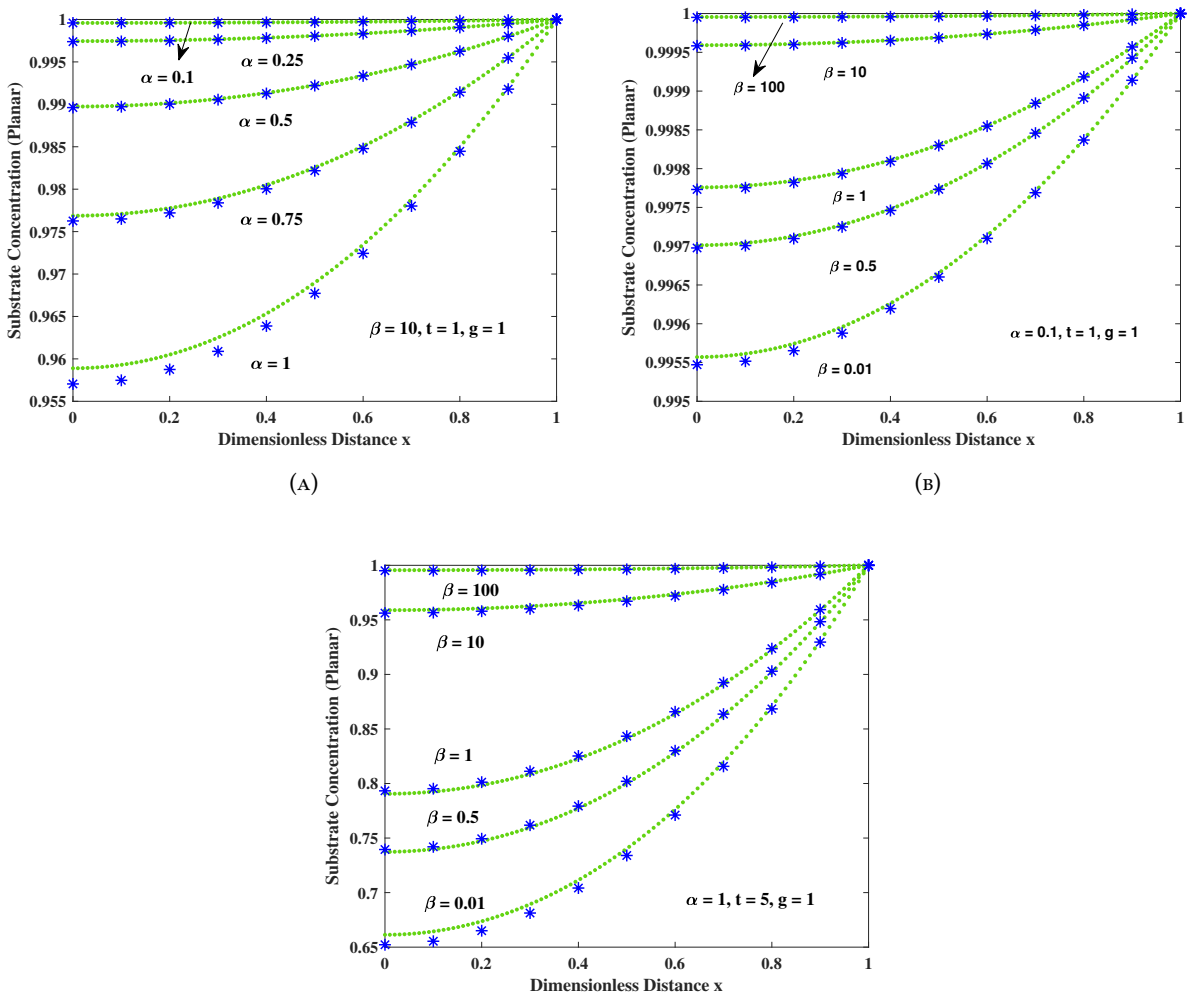

(A) (B)

(C)

FIGURE 1. Comparison graph of Dimensionless substrate concentration $C(x,t)$ versus the dimensionless distance x (1a) for the fixed parametric values $\beta = 10, t = 1$ and for various values of α, (1b) for the fixed parametric values $\alpha = 0.1, t = 1$ and for various values of β, (1c) for the fixed parametric values $\alpha = 1, t = 5$ and for various values of β, where '$\cdots$' represents the numerical results and '$***$' represents the analytical results by HPM Eq. (4.1) for planar pellets.

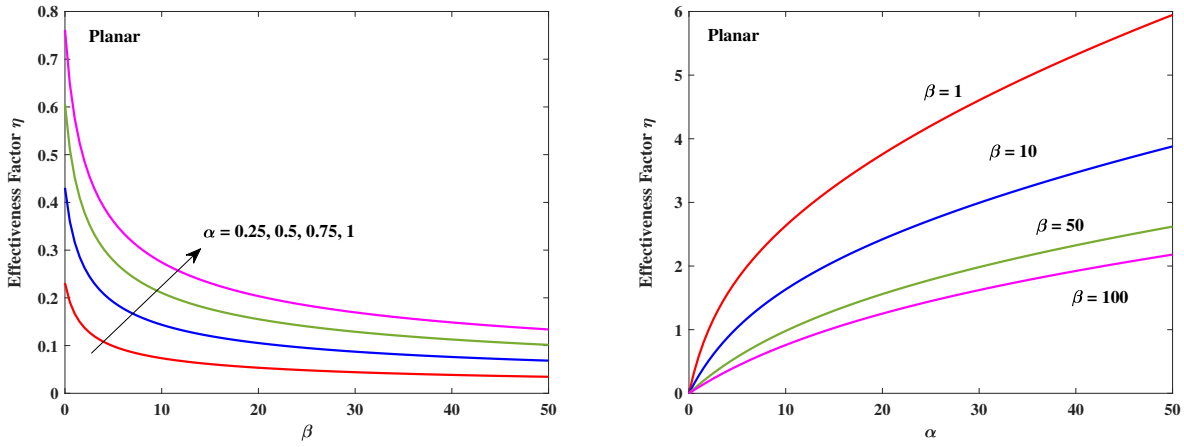

(A) (B)

FIGURE 2. Effectiveness factor for (2a) various values of Thiele modulus α vs Michaelis-Menten constant β and (2b) for various values of Michaelis-Menten constant β vs Thiele modulus α.

TABLE 1. Comparison table of the approximate analytical results by HPM with the corresponding numerical results for fixed values of parameters α, t and for various values of β for planar geometry.

	$\alpha = 0.4, \beta$=1, t=10			α=0.4, β=5, t=10			α=0.4, β=10, t=10		
x	Numerical	HPM Eq.(4.1)	Error	Numerical	HPM Eq.(4.1)	Error	Numerical	HPM Eq.(4.1)	Error
0	0.96070	0.96130	0.06245	0.98670	0.98680	0.01013	0.99270	0.99280	0.01007
0.2	0.96227	0.96284	0.05924	0.98723	0.98733	0.00957	0.99299	0.99309	0.00988
0.4	0.96698	0.96746	0.04991	0.98883	0.98891	0.00791	0.99386	0.99396	0.00931
0.6	0.97483	0.97518	0.03535	0.99149	0.99154	0.00532	0.99532	0.99540	0.00841
0.8	0.98585	0.98601	0.01702	0.99521	0.99523	0.00204	0.99735	0.99742	0.00727
1	1.00004	1.00001	0.00311	1.00001	0.99999	0.00158	0.99997	1.00003	0.00599
	Average Error		0.03785	Average Error		0.00609	Average Error		0.00849

5.2. **Cylindrical geometry.** For the pellet shape factor value g = 2, the pellet geometry becomes a cylindrical one and if we apply this factor value in Eq. (3.1) and Eq. (3.2), we have the non-steady state concentration Eq. (4.3) and its corresponding effectiveness factor Eq. (4.4) under this geometry. The dimensionless concentration profiles according to the cylindrical geometrical results so obtained have clearly been demonstrated by the graphs given below and the approximate analytical results obtained by the HPM have been compared with their numerical simulation graphs plotted with the help of MATLAB software coding for various values of the parameters α, β and the time factor t to have a sense of ensuring how far our method of solution yields results

coherent to the numerical simulations. Here also we have a clear vision that the approximate analytical results even in non-steady state are almost coinciding with the results of numerical simulations. In Table. 2, the mean errors have been calculated between the analytical solutions and the numerical solutions for the various parameter values which have been collected from the previous works and it describes that the approximate analytical solutions and the corresponding numerical results almost coincide under this geometry even in non-steady state. The dimensionless concentration levels and the overall effectiveness factor variations corresponding to the variations in concentration levels have been represented by the graphs, Figure. 3 and Figure. 4, under various values of the parameters by this geometry, with the help of MATLAB coding, that satisfies the characteristics of flows as per the Michaelis-Menten kinetics and the Fick's laws.

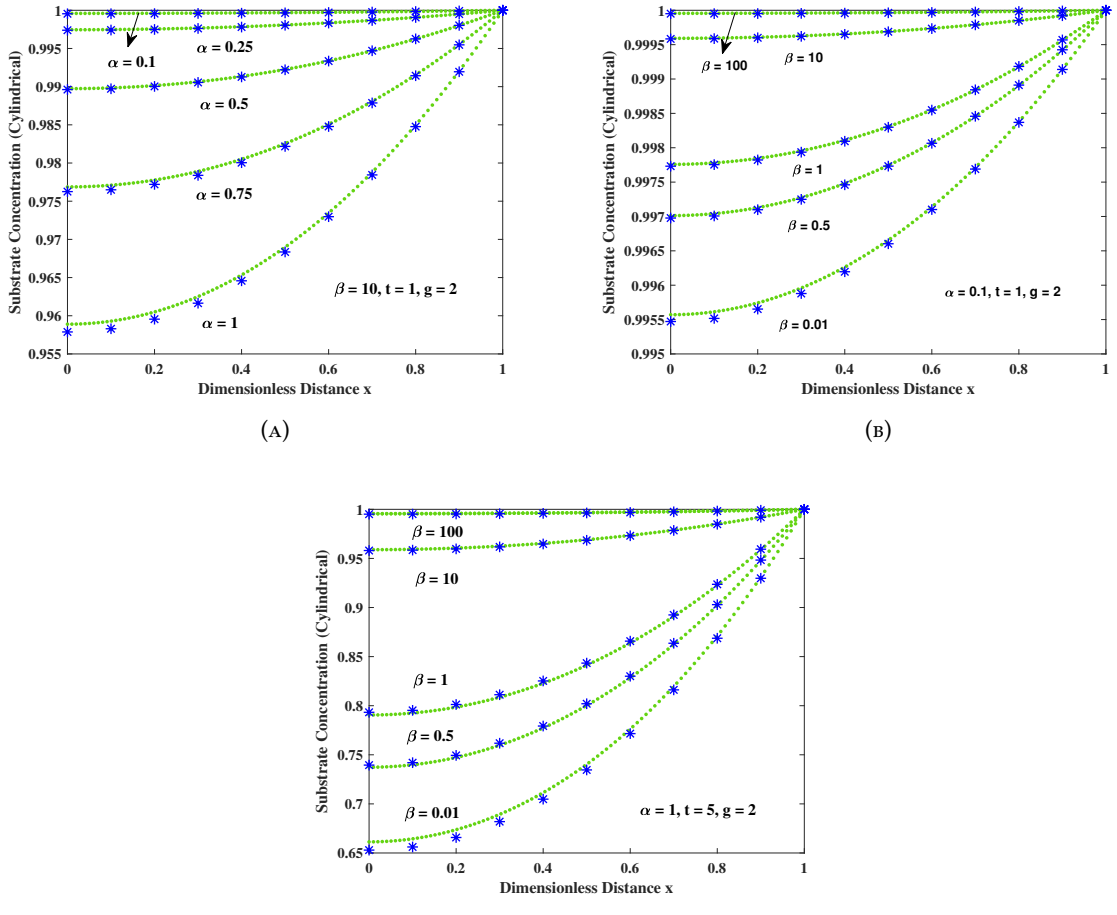

FIGURE 3. Comparison graph of Dimensionless substrate concentration $C(x,t)$ versus the dimensionless distance x (3a) for the fixed parametric values $\beta = 10, t = 1$ and for various values of α, (3b) for the fixed parametric values $\alpha = 0.1, t = 1$ and for various values of β, (3c) for the fixed parametric values $\alpha = 1, t = 5$ and for various values of β, where '$\cdots$' represents the numerical results and '$***$' represents the analytical results by HPM Eq. (4.3) for cylindrical pellets.

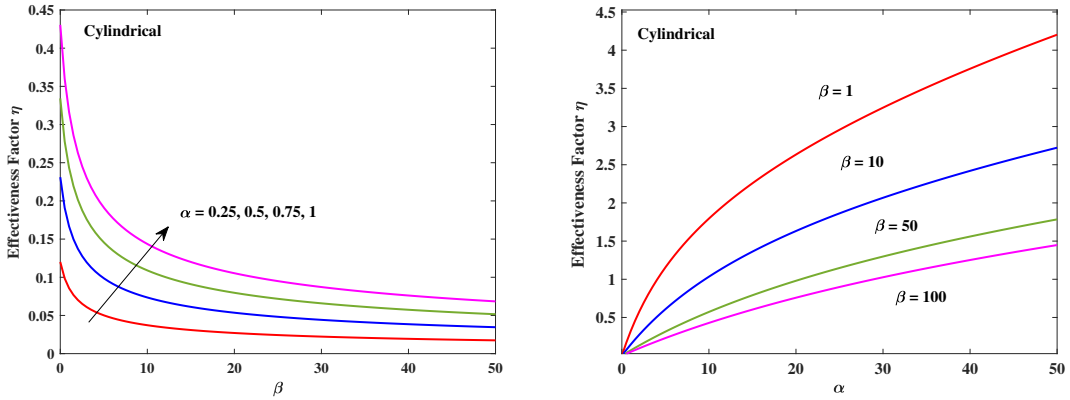

(A) (B)

FIGURE 4. Effectiveness factor for (4a) various values of Thiele modulus α vs Michaelis-Menten constant β and (4b) for various values of Michaelis-Menten constant β vs Thiele modulus α.

TABLE 2. Comparison table of the approximate analytical results by HPM with the corresponding numerical results for fixed values of parameters α, t and for various values of β for cylindrical geometry.

	$\alpha = 0.4, \beta$=1, t=10			α=0.4, β=5, t=10			α=0.4, β=10, t=10		
x	Numerical	HPM Eq.(4.3)	Error	Numerical	HPM Eq.(4.3)	Error	Numerical	HPM Eq.(4.3)	Error
0	0.96070	0.96130	0.06245	0.98670	0.98680	0.01013	0.99270	0.99280	0.01007
0.2	0.96227	0.96284	0.05924	0.98723	0.98733	0.00957	0.99299	0.99309	0.00988
0.4	0.96698	0.96746	0.04991	0.98883	0.98891	0.00791	0.99386	0.99396	0.00931
0.6	0.97483	0.97518	0.03535	0.99149	0.99154	0.00532	0.99532	0.99540	0.00841
0.8	0.98585	0.98601	0.01702	0.99521	0.99523	0.00204	0.99735	0.99742	0.00727
1	1.00004	1.00001	0.00311	1.00001	0.99999	0.00158	1.00000	1.00003	0.00287
	Average Error		0.03785	Average Error		0.00609	Average Error		0.00797

5.3. **Spherical geometry.** When we apply g = 3, the pellet geometry would be of a spherical one and if we substitute this factor value in Eq. (3.1) and Eq. (3.2), we have the non-steady state concentration Eq. (4.5) and its corresponding effectiveness factor Eq. (4.6) under this geometry. The dimensionless concentration profiles according to the spherical geometrical results so obtained have clearly been exhibited by the graphs given below and the approximate analytical results obtained by the HPM have been compared with their numerical simulation graphs plotted with the help of MATLAB software for various values of the parameters α, β and the time factor t to have a sense of ensuring how far our method of solution yields results much coherent to the numerical simulations. In view of the comparison manner, we could have a clear vision that the

approximate analytical results even in non-steady state are almost coinciding with the results of numerical simulations. In Table. 3, the mean errors have been calculated between the analytical solutions and the numerical solutions for the three sets of parameter values which have been collected from the previous articles and it describes that the approximate analytical solutions and the corresponding numerical results almost coincide under this geometry even in non-steady state. The dimensionless concentration levels and the overall effectiveness factors in different concentration levels have been represented by the graphs, Figure. 5 and Figure. 6, under various values of the parameters in this geometry, with the help of MATLAB coding, that satisfies the characteristics of flows as per the Michaelis-Menten kinetics and the Fick's laws.

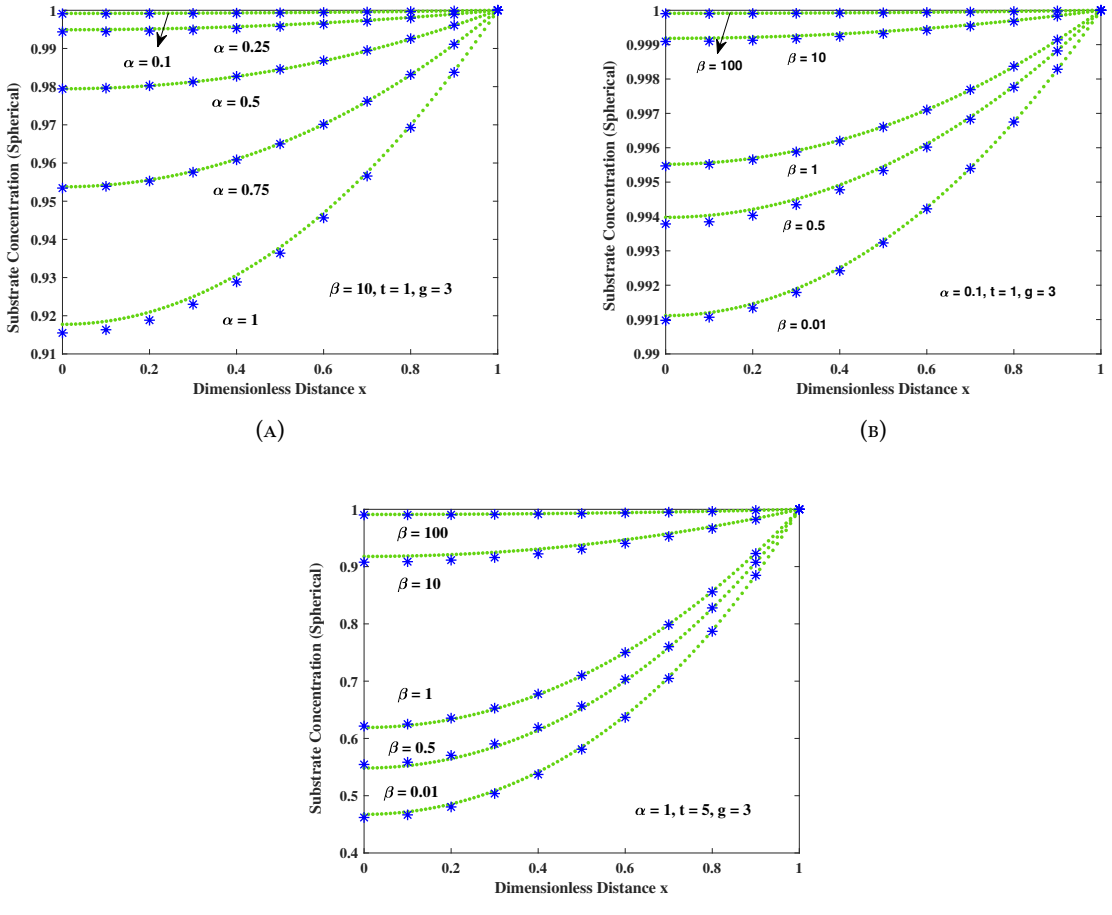

FIGURE 5. Comparison graph of Dimensionless substrate concentration $C(x,t)$ versus the dimensionless distance x (5a) for the fixed parametric values $\beta = 10, t = 1$ and for various values of α, (5b) for the fixed parametric values $\alpha = 0.1, t = 1$ and for various values of β, (5c) for the fixed parametric values $\alpha = 1, t = 5$ and for various values of β, where '$\cdots$' represents the numerical results and '$***$' represents the analytical results by HPM Eq. (4.5) for spherical pellets.

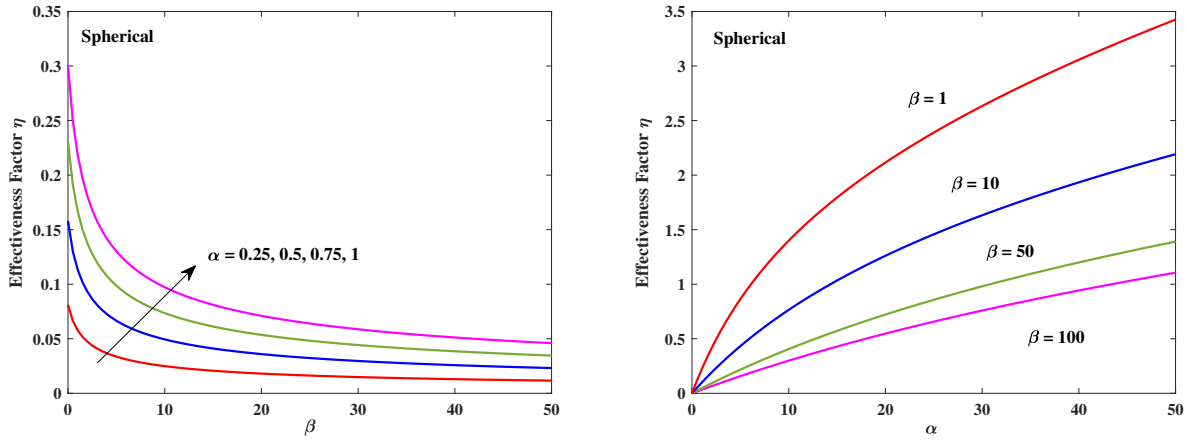

(A) (B)

FIGURE 6. Effectiveness factor for (6a) various values of Thiele modulus α vs Michaelis-Menten constant β and (6b) for various values of Michaelis-Menten constant β vs Thiele modulus α.

TABLE 3. Comparison table of the approximate analytical results by HPM with the corresponding numerical results for fixed values of parameters α, t and for various values of β for spherical geometry.

	$\alpha = 0.4, \beta$=1, t=10			α=0.4, β=5, t=10			α=0.4, β=10, t=10		
x	Numerical	HPM Eq.(4.5)	Error	Numerical	HPM Eq.(4.5)	Error	Numerical	HPM Eq.(4.5)	Error
0	0.92270	0.92500	0.24927	0.97590	0.97390	0.20494	0.9855	0.98560	0.01015
0.2	0.92577	0.92796	0.23648	0.97690	0.97500	0.19449	0.98608	0.98617	0.00938
0.4	0.93500	0.93687	0.19953	0.97970	0.97810	0.16332	0.98783	0.98790	0.00713
0.6	0.95041	0.95177	0.14249	0.98450	0.98330	0.12189	0.99073	0.99077	0.00360
0.8	0.97207	0.97277	0.07186	0.99120	0.99060	0.06053	0.99480	0.99479	0.00088
1	1.00003	0.99999	0.00394	1.00000	1.0000	0.00000	1.00003	0.99998	0.00586
	Average Error		0.15059	Average Error		0.12419	Average Error		0.00616

6. SENSITIVITY OF PARAMETERS

Derivatives of the system with respect to the parameters quantify the effect of the parameters on the solution of the system. The obtained results of parametric sensitivity analysis reveal the amount of parametric impact on the effectiveness of batch reactor performance. Figure. 7 symbolizes the influence of the effect on the effectiveness of the reaction diffusion process of the enzymatic reaction inside the batch reactor. The parametric values utilized for the analysis are $\alpha = 0.6$, $\beta = 5$.

From Figure. 7, it is seen that the Thiele modulus has the most effect on the effective working of the batch reactor with 95%, and the dimensionless Michaelis-Menten constant has the least impact on the effectiveness factor of the batch reactor with 5%.

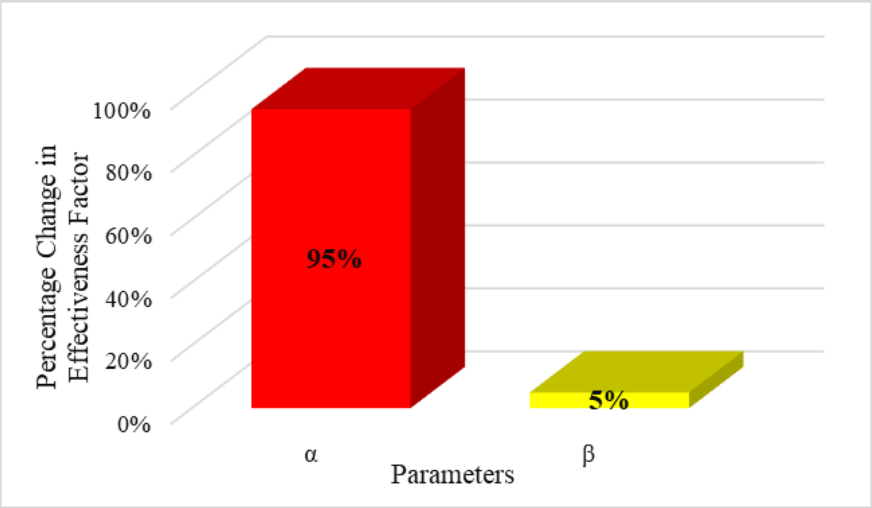

FIGURE 7. Effect of parameters on effectiveness factor

7. CONCLUSION

The non-steady-state model of immobilized enzyme on the nonporous material is mathematically analyzed in this paper. The closed-form approximate analytical expression for the non-linear non-steady-state reaction-diffusion equation of substrate concentration with the non-linear terms related to Michaelis-Menten kinetics and the effectiveness factor are obtained using HPM. The analytical expressions are obtained for substrate concentration and effectiveness factor for the planar, cylindrical and spherical geometric enzymatic pellets. The obtained analytical expression is compared with the numerical solution obtained using the MATLAB software, yield satisfactory agreement for all values of the parameters. The effect of the parameters on the effectiveness factor of the batch reactor is also analysed. It is found out that the Thiele modulus α has the maximum effect on the effectiveness factor of the system.

The proposed non-steady-state result is utilized to investigate the effect of various diffusion and kinetic parameters on the substrate and the effectiveness factor of the system. The above proposed method can be employed to solve the time-dependent reaction-diffusion problems arising in the various fields of chemistry.

8. APPENDIX-A: OBTAINING THE APPROXIMATE ANALYTICAL SOLUTION OF EQUATION (2.1) USING HPM

By constructing the homotopy for the Eq. (2.1), we have

$$(1-p)\left[\frac{\partial C}{\partial t}-\frac{\partial^2 C}{\partial x^2}-\frac{g-1}{x}\frac{\partial C}{\partial x}+\frac{\alpha^2 C}{1+\beta C(1,t)}\right]+p\left[\frac{\partial C}{\partial t}-\frac{\partial^2 C}{\partial x^2}-\frac{g-1}{x}\frac{\partial C}{\partial x}+\frac{\alpha^2 C}{1+\beta C}\right]=0 \qquad (8.1)$$

Applying the initial condition Eq. (2.2) in Eq. (8.1), we get

$$(1-p)\left[\frac{\partial C}{\partial t}-\frac{\partial^2 C}{\partial x^2}-\frac{g-1}{x}\frac{\partial C}{\partial x}+\frac{\alpha^2 C}{1+\beta}\right]+p\left[\frac{\partial C}{\partial t}-\frac{\partial^2 C}{\partial x^2}-\frac{g-1}{x}\frac{\partial C}{\partial x}+\frac{\alpha^2 C}{1+\beta C}\right]=0 \tag{8.2}$$

Then we shall obtain the approximate solution in the form

$$C = C_0 + pC_1 + p^2C_2 + \cdots \tag{8.3}$$

Substituting Eq. (8.3) in Eq. (8.2) and equating the coefficients of the zeroth power of p, we have

$$\frac{\partial C_0}{\partial t}-\frac{\partial^2 C_0}{\partial x^2}-\frac{g-1}{x}\frac{\partial C_0}{\partial x}+aC_0=0 \tag{8.4}$$

where $a=\frac{\alpha^2}{1+\beta}$. Taking Laplace transform on Eq. (8.4), we have

$$\frac{d^2\tilde{C}_0(x,s)}{dx^2}+\frac{g-1}{x}\frac{d\tilde{C}_0(x,s)}{dx}-(s+a)\tilde{C}_0(x,s)=0 \tag{8.5}$$

with the corresponding boundary conditions,

$$\frac{d\tilde{C}_0(x,s)}{dx}=0 \text{ when } x=0, \tag{8.6}$$

$$\tilde{C}_0(x,s)=\frac{1}{s} \text{ when } x=1. \tag{8.7}$$

where $\tilde{C}_0(x,s)$ is the Laplace transform of $C_0(x,s)$. Then by AGM, assuming a solution of the above equation Eq. (8.5), satisfying the corresponding initial and boundary conditions Eq. (8.6), that

$$\tilde{C}_0(x,s)=A_0\cosh(mx)+B_0\sinh(mx) \tag{8.8}$$

where $A_0=\frac{1}{s\cosh m}$ and $B_0=0$, we obtain the solution of the above system Eqs. (8.5) - (8.6) as

$$\tilde{C}_0(x,s)=\frac{\cosh(mx)}{s\cosh m} \tag{8.9}$$

Applying Eq. (8.9) in Eq. (8.5), and substituting $x=1$, we have

$$m^2+(g-1)\,m\tanh m\,-(s+a)=0 \tag{8.10}$$

As we have that for sufficiently small m values, $\tanh m \approx m$, we get the value of m as

$$m=\sqrt{\frac{s+a}{g}} \tag{8.11}$$

Substituting this in Eq. (8.9), we obtain the solution of Eq. (8.5) as

$$\tilde{C}_0(x,s)=\frac{\cosh\left(x\sqrt{\frac{s+a}{g}}\right)}{s\cosh\left(\sqrt{\frac{s+a}{g}}\right)} \tag{8.12}$$

The residues of Eq. (8.12) can be obtained at $s=0$, we obtain a simple pole and the solution of $\cosh\left(\sqrt{\frac{s+a}{g}}\right)=0$ generates infinitely many poles given by $s_n=-g\frac{(2n+1)^2\pi^2}{4}-ga$, where n = 0, 1, 2,. . . .

$$\text{Res}\left[\frac{\cosh\left(x\sqrt{\frac{s+a}{g}}\right)}{s\cosh\left(\sqrt{\frac{s+a}{g}}\right)}\right]=\left[\frac{\cosh\left(x\sqrt{\frac{s+a}{g}}\right)}{s\cosh\left(\sqrt{\frac{s+a}{g}}\right)}\right]_{s=0}+\left[\frac{\cosh\left(x\sqrt{\frac{s+a}{g}}\right)}{s\cosh\left(\sqrt{\frac{s+a}{g}}\right)}\right]_{s=s_n} \tag{8.13}$$

The residue at $s = 0$ is given by

$$\text{Res}\left[\frac{\cosh\left(x\sqrt{\frac{s+a}{g}}\right)}{s\cosh\left(\sqrt{\frac{s+a}{g}}\right)}\right]_{s=0}=\frac{\cosh\left(x\sqrt{\frac{a}{g}}\right)}{\cosh\left(\sqrt{\frac{a}{g}}\right)} \tag{8.14}$$

and the residue at $s = s_n$ is given by

$$\text{Res}\left[\frac{\cosh\left(x\sqrt{\frac{s+a}{g}}\right)}{s\cosh\left(\sqrt{\frac{s+a}{g}}\right)}\right]_{s=s_n}=-\pi\sum_{n=0}^{\infty}\frac{(2n+1)\cos\left(\frac{(2n+1)\pi}{2}x\right)e^{-gt\left(\frac{(2n+1)^2\pi^2}{4}+a\right)}}{\left(\frac{(2n+1)^2\pi^2}{4}+a\right)\sin\left(\frac{(2n+1)\pi}{2}\right)} \tag{8.15}$$

Substrate concentration can be obtained by adding Eqs. (8.15) and (8.14) as shown in Eq. (3.1).

Conflicts of Interest: The authors declare that there are no conflicts of interest regarding the publication of this paper.

References

[1] L. Goldstein, Kinetic Behavior of Immobilized Enzyme Systems, Methods Enzymol. (1976), 397–443. https://doi.org/10.1016/s0076-6879(76)44031-4.

[2] T. Kobayashi, K.J. Laidler, Kinetic Analysis for Solid-Supported Enzymes, Biochim. Biophys. Acta (BBA) - Enzymol. 302 (1973), 1–12. https://doi.org/10.1016/0005-2744(73)90002-8.

[3] A. Kheirolomoom, S. Katoh, E. Sada, K. Yoshida, Reaction Characteristics and Stability of a Membrane-bound Enzyme Reconstituted in Bilayers of Liposomes, Biotech. Bioeng. 37 (1991), 809–813. https://doi.org/10.1002/bit.260370904.

[4] S. Gondo, S. Isayama, K. Kusunoki, Effects of Internal Diffusion on the Lineweaver-Burk Plots for Immobilized Enzymes, Biotech. Bioeng. 17 (1975), 423–431. https://doi.org/10.1002/bit.260170310.

[5] D.J. Fink, T. Na, J.S. Schultz, Effectiveness Factor Calculations for Immobilized Enzyme Catalysts, Biotech. Bioeng. 15 (1973), 879–888. https://doi.org/10.1002/bit.260150505.

[6] M.D. Benaiges, C. Solà, C. De Mas, Intrinsic Kinetic Constants of an Immobilised Glucose-isomerase, J. Chem. Tech. Biotech. 36 (1986), 480–486. https://doi.org/10.1002/jctb.280361008.

[7] O.M. Kirthiga, M. Sivasankari, R. Vellaiammal, L. Rajendran, Theoretical Analysis of Concentration of Lactose Hydrolysis in a Packed Bed Reactor Using Immobilized β-Galactosidase, Ain Shams Eng. J. 9 (2018), 1507-1512. https://doi.org/10.1016/j.asej.2016.10.007.

[8] T. Praveen, P. Valencia, L. Rajendran, Theoretical Analysis of Intrinsic Reaction Kinetics and the Behavior of Immobilized Enzymes System for Steady-State Conditions, Biochem. Eng. J. 91 (2014), 129–139. https://doi.org/10.1016/j.bej.2014.08.001.

[9] P. Jeyabarathi, L. Rajendran, M. Abukhaled, M. Kannan, Semi-Analytical Expressions for the Concentrations and Effectiveness Factor for the Three General Catalyst Shapes, React. Kinet. Mech. Catal. 135 (2022), 1739–1754. https://doi.org/10.1007/s11144-022-02205-x.

[10] M. Sivakumar, R. Senthamarai, L. Rajendran, M.E.G. Lyons, Reaction and Kinetic studies of Immobilized Enzyme Systems: Part-I Without External Mass Transfer Resistance, Int. J. Electrochem. Sci. 17 (2022), 221159. https://doi.org/10.20964/2022.09.69.

[11] M. Sivakumar, R. Senthamarai, L. Rajendran, M.E.G. Lyons, Reaction and Kinetic studies of Immobilized Enzyme Systems: Part-II With External Mass Transfer Resistance, Int. J. Electrochem. Sci. 17 (2022) 221031. https://doi.org/10.20964/2022.10.43.

[12] S.A. Mireshghi, A. Kheirolomoom, F. Khorasheh, Application of an Optimization Algorithm for Estimation of Substrate Mass Transfer Parameters for Immobilized Enzyme Reactions, Sci. Iran. 3 (2001), 189–196.

[13] J.H. He, Homotopy perturbation technique, Comput. Methods Appl. Mech. Eng. 178 (1999), 257–262. https://doi.org/10.1016/s0045-7825(99)00018-3.

[14] J.H. He, M.L. Jiao, K.A. Gepreel, Y. Khan, Homotopy Perturbation Method for Strongly Nonlinear Oscillators, Math. Comput. Simul. 204 (2023), 243–258. https://doi.org/10.1016/j.matcom.2022.08.005.

[15] R. Senthamarai, R. Jana Ranjani, Solution of Non-Steady-State Substrate Concentration in the Action of Biosensor Response at Mixed Enzyme Kinetics, J. Phys.: Conf. Ser. 1000 (2018), 012138. https://doi.org/10.1088/1742-6596/1000/1/012138.

[16] M. Sivakumar, R. Senthamarai, Mathematical Model of Epidemics: Analytical Approach to Sirw Model Using Homotopy Perturbation Method, AIP Conf. Proc. 2277 (2020), 130009. https://doi.org/10.1063/5.0025502.

[17] M.R. Akbari, D.D. Ganji, A. Majidian, A.R. Ahmadi, Solving Nonlinear Differential Equations of Vanderpol, Rayleigh and Duffing by AGM, Front. Mech. Eng. 9 (2014), 177–190. https://doi.org/10.1007/s11465-014-0288-8.

[18] P. Jeyabarathi, L. Rajendran, M.E.G. Lyons, M. Abukhaled, Theoretical Analysis of Mass Transfer Behavior in Fixed-Bed Electrochemical Reactors: Akbari-Ganji's Method, Electrochem. 3 (2022), 699–712. https://doi.org/10.3390/electrochem3040046.

[19] M.A. Attar, M. Roshani, Kh. Hosseinzadeh, D.D. Ganji, Analytical Solution of Fractional Differential Equations by Akbari-Ganji's Method, Part. Differ. Equ. Appl. Math. 6 (2022), 100450. https://doi.org/10.1016/j.padiff.2022.100450.

[20] M. Mallikarjuna, R. Senthamarai, An Amperometric Biosensor and Its Steady State Current in the Case of Substrate and Product Inhibition: Taylors Series Method and Adomian Decomposition Method, J. Electroanal. Chem. 946 (2023), 117699. https://doi.org/10.1016/j.jelechem.2023.117699.

[21] C.H. He, Y. Shen, F.Y. Ji, J.H. He, Taylor Series Solution for Fractal Bratu-Type Equation Arising in Electrospinning Process, Fractals. 28 (2020), 2050011. https://doi.org/10.1142/s0218348x20500115.

[22] A. Afreen, A. Raheem, Study of a Nonlinear System of Fractional Differential Equations with Deviated Arguments Via Adomian Decomposition Method, Int. J. Appl. Comput. Math. 8 (2022), 269. https://doi.org/10.1007/s40819-022-01464-5.

[23] M. Mallikarjuna, R. Senthamarai, Analytical Solution of Enzyme Catalysis in Calcium Alginate Beads, AIP Conf. Proc. 2516 (2022), 250007. https://doi.org/10.1063/5.0108653.

[24] T. Vijayalakshmi, R. Senthamarai, Application of Homotopy Perturbation and Variational Iteration Methods for Nonlinear Imprecise Prey–predator Model With Stability Analysis, J. Supercomput. 78 (2021), 2477–2502. https://doi.org/10.1007/s11227-021-03956-5.

[25] G.H. Ibraheem, M. Turkyilmazoglu, M.A. AL-Jawary, Novel Approximate Solution for Fractional Differential Equations by the Optimal Variational Iteration Method, J. Comput. Sci. 64 (2022), 101841. https://doi.org/10.1016/j.jocs.2022.101841.